Marine Pollution Bulletin 131 (2018) 17–21

Contents lists available at ScienceDirect

Marine Pollution Bulletin

journal homepage: www.elsevier.com/locate/marpolbul

# Tissue-specific metabolic responses of the pearl oyster *Pinctada martensii* exposed to benzo[*a*]pyrene

Hao Chen[a,b,1], Xiaoping Diao[a,b,*], Hailong Zhou[a,b,*]

[a] State Key Laboratory of Marine Resource Utilization in South China Sea, Hainan University, Haikou 570228, China
[b] Institute of Tropical Agriculture and Forestry, Hainan University, Haikou 570228, China

ARTICLE INFO

*Keywords:*
Benzo[*a*]pyrene
*Pinctada martensii*
Metabolomics
$^{1}$H NMR
Biomarker

ABSTRACT

Benzo[*a*]pyrene (BaP) is a polycyclic aromatic hydrocarbon (PAH) that is well known for its teratogenic, mutagenic and carcinogenic effects. In this study, we applied metabolomics to investigate the tissue-specific metabolic responses of the *Pinctada martensii* digestive glands and gills after a short-duration exposure to BaP (1 μg/L and 10 μg/L). After 72 h of exposure to BaP, the majority of metabolite changes were related to osmolytes, energy metabolites, and amino acids. BaP (1 μg/L) accelerated energy deterioration and decreased osmotic regulation, while BaP (10 μg/L) disturbed energy metabolism and increased osmotic stress in the digestive glands. Both BaP doses disturbed osmotic regulation and energy metabolism in the gills. BaP also induced neurotoxicity in both tissues. These findings demonstrated that BaP exhibited tissue-specific metabolic responses in *P. martensii*. The difference in these metabolite responses between the digestive glands and gills might prove to be suitable biomarkers for indicating exposure to specific marine pollutants.

## 1. Introduction

Benzo[*a*]pyrene (BaP) is a polycyclic aromatic hydrocarbon (PAH) and has strong mutagenic, teratogenic, and carcinogenic effects on various species (Yan et al., 2010; Tung et al., 2014; Santacroce et al., 2015). Furthermore, BaP has a high affinity for sediment in the aquatic environment, where it can persist and act as a mutagenic agent (Phillips, 1999; Wills et al., 2010). Some researchers have particularly reported the genotoxic effects of BaP on zebra mussel (*Dreissena polymorpha*) (Binelli et al., 2008). Other studies also demonstrated the induced behavior effects of zebrafish embryos (Knecht et al., 2017) and CYP1A induction and morphological changes in Mediterranean blue mussel (*Mytilus galloprovincialis*) (Speciale et al., 2018).

Metabolomics is the study of endogenous, low molecular weight metabolites within a cell or tissue (Viant, 2007). This systems-based approach can reveal the mechanisms of metabolic reactions induced by contaminants by comparing the profiles of metabolomes in normal organisms (Tuffnail et al., 2008; Watanabe et al., 2015; Cappello et al., 2016b; Chiu et al., 2017). Previously, Zhang et al. (2011a) successfully utilized nuclear magnetic resonance (NMR)-based metabolomics to investigate BaP induced hormesis phenomenon in clams (*Ruditapes philippinarum*). The metabolic changes in osmolytes, amino acids, energy metabolites and neurotransmitters of undermussels (*Mytilus galloprovincialis*) under exposure to PAHs were also determined using the same technique (Cappello et al., 2013). These results indicated that NMR-based metabolomics is a powerful tool to elucidate PAH pollution-induced toxic effects on organisms.

The pearl oyster *Pinctada martensii*, a commonly used shellfish for economically producing pearls, is mainly found in subtropical and tropical oceans (Shi et al., 2013). In our previous research, *P. martensii* was shown to be an applicable indicator organism for marine pollution due to its high propensity for bioaccumulation (Wang et al., 2017; Xie et al., 2017). The digestive glands and gills are the important target organs of marine bivalves that can accumulate pollutants (Canesi et al., 2010; Fernandez-Tajes et al., 2011; Banni et al., 2014; Dorts et al., 2014). In this study, we selected the tissues of these two target organs of *P. martensii* to investigate the tissue-specific effects of BaP via $^{1}$H NMR-based metabolomics.

## 2. Materials and methods

### 2.1. Animals and experimental design

Adult *P. martensii* (shell length 6.78 ± 0.35 cm, aged 2 years, $n = 120$) were collected from a site in Li'an Bay (Hainan, China) in spring. Pearl oysters were acclimatized in aerated sand-filtered

* Corresponding authors at: Institute of Tropical Agriculture and Forestry, Hainan University, Haikou 570228, Hainan, China.
*E-mail addresses:* diaoxip@hainu.edu.cn (X. Diao), zhouhl@hainu.edu.cn (H. Zhou).
[1] Institute of Tropical Agriculture and Forestry, Hainan University, Haikou 570228, Hainan, China.

https://doi.org/10.1016/j.marpolbul.2018.03.057
Received 14 September 2017; Received in revised form 22 March 2018; Accepted 29 March 2018

seawater (salinity 32‰; pH 8.2 ± 0.1; temperature 27 ± 1 °C) for 7 days in the laboratory. Throughout the periods of acclimation *P. martensii* were fed with the marine microalgae *Tetraselmis chui* at a ration of 2% of tissue per dry weight daily. The samples were randomly divided into four groups of 30 oysters per 40 L tank. One group cultured in seawater was used as seawater control. Another group cultured in seawater with 0.001% acetone (v/v) was used as solvent control group. The other two groups were exposed to BaP (1 μg/L and 10 μg/L) dissolved in acetone at the final concentration of 0.001%. The concentrations of BaP used in the experiments were determined according to pre-experiment and previous report (Chen et al., 2016). The pearl oysters were fasted, and the seawater was renewed once every day during the exposure periods. After a 72-h exposure, the tissues of the digestive glands and gills of 12 individuals from each group were dissected. All the tissues were flash-frozen in liquid nitrogen and remained frozen until metabolite extraction.

### 2.2. Metabolite extraction

Polar metabolites in the tissues of *P. martensii* were extracted using a modified protocol (Wu et al., 2008). Briefly, the digestive glands and gills (approximately 100 mg) were homogenized and extracted in a solvent mixture of methanol:chloroform:water (400 μL: 200 μL: 85 μL). The tissue extracts were subsequently dissolved in 600 μL of phosphate buffer [100 mM $NaH_2PO_4$ and $Na_2HPO_4$ with 0.5 mM sodium 3-trimethlysilyl-2, 2, 3, 3-$d_4$-propionate (TSP), pH 7.0] in $D_2O$. The mixture was vortexed and centrifuged at 3000*g* for 5 min at 4 °C. A total volume of 550 μL supernatant substance was pipetted into a 5 mm NMR tube for subsequent NMR analysis.

### 2.3. $^1H$ NMR spectroscopy and data analysis

Extracted metabolites were analyzed using the NMR spectrometer (500.18 MHz, at 298 K) (BioSpin AV500, Bruker, Switzerland). One-dimensional (1D) spectra were acquired using an 11.9 μs pulse, 0.1 s mixing time, and 3.0 s relaxation delay with a standard 1D NOESY pulse sequence. All spectra were recorded using a spectral width of 6009.6 Hz, and 128 transients collected with 16,384 data points (Liu et al., 2011). All $^1H$ NMR spectra were phased, baseline-corrected, and calibrated (TSP at 0.0 ppm) using TopSpin (version 2.1, Bruker) (Zhang et al., 2011b). The chemical shifts of metabolites were analyzed using Chenomx Suite (Evaluation Version, Chenomx, Inc., Canada) to identify the major metabolites (Viant et al., 2003).

Multivariate data analysis was performed using SIMCA-$P^+$ (V11.0, Umetric, Sweden). In this study, supervised partial least squares discriminant analysis (PLS-DA) and orthogonal projection to latent structure with discriminant analysis (O-PLS-DA) were sequentially performed to reveal the statistically significant metabolite responses induced by BaP exposure.

The results were visualized in terms of the scores plotted to show the classifications and corresponding loadings plots of the NMR spectral variables contributing to the classifications. The model coefficients were calculated from the coefficients incorporating the weight of the variables in order to enhance the interpretability of the model. Subsequently, the metabolic differences responsible for the classifications between the solvent control group and BaP-exposed groups could be detected in the coefficient-coded loadings plots. The coefficient plots were generated using Matlab (V7.0, the Math Works Inc., Natwick, USA). The correlation coefficient was determined according to the test for the significance of the Pearson's product-moment correlation coefficient. The $R^2$ in the permutated plot described how well the data fit the derived model. $Q^2$ describes the predictive ability of the derived model and provides a measure of the model quality (Feng et al., 2013).

## 3. Results and discussion

### 3.1. $^1H$ NMR spectroscopy of the digestive gland and gill extracts of *P. martensii*

Certain prominent metabolites were distinguished in the digestive glands and gills (See Supplementary Fig. S1). These metabolites were classified as organic osmolytes (taurine, hypotaurine, betaine, homarine, dimethylglycine and glycine), amino acids (e.g., valine, isoleucine, leucine), citric acid cycle intermediates (succinate and malonate), and energy storage compounds (glucose and adenosine triphosphate (ATP)). Several metabolites were identified in different tissue extracts. Specifically, glycogen, nicotinamide adenine dinucleotide phosphate ($NADP^+$), and phenylalanine were identified in the digestive gland tissue extracts, and fumarate was only detected in the gill tissue extracts. However, all spectra were dominated by the critical organic osmolyte taurine.

### 3.2. Effects of BaP on the metabolome of the digestive glands and gills

After being exposed to BaP for 72 h, O-PLS-DA analysis indicated that both BaP treatments (1 μg/L and 10 μg/L) significantly altered some metabolites ($P < 0.05$) in the digestive gland and gill tissues, as shown in Figs. 1 and 2.

#### 3.2.1. Effects of BaP on the metabolome of digestive glands

In terms of metabolites of the digestive glands, the level of glutamate was significantly increased by the low concentration of BaP-exposed treatment, while the levels of branched chain amino acids (BCAAs) (valine, isoleucine, leucine), taurine, glycine, glucose, inosine, tyrosine, histidine, and phenylalanine were significantly decreased. Simultaneously, the levels of homarine and ATP were significantly elevated with high BaP-exposure treatment, whereas the levels of BCAAs, taurine, glycine, glucose, inosine, tyrosine, histidine, phenylalanine, glutamate, threonine, and arginine were dramatically reduced (Fig. 1 and Table 1).

Amino acids are involved in energy metabolism, osmotic regulation, and other essential life processes (Viant et al., 2003). The lower levels of tyrosine, histidine, phenylalanine, and arginine clearly indicated that BaP induced energy metabolism disorders. The concentration of arginine correlates with ATP/adenosine diphosphate (ADP) levels in invertebrates (Fasulo et al., 2012). The decreased arginine level suggested that a high dose of BaP disrupted energy metabolism occurring in the urea cycle.

Glutamate is involved in multiple physiological functions and plays a key role in cellular metabolism (Newsholme et al., 2003). Excessive accumulation of glutamate cause glutamate neurotoxicity, induces neuronal over-activation and ultimately leads to cell death (Liu et al., 2015; Cappello et al., 2016a). Similarly, glycine can produce neuronal stimulation and neurotoxicity and is associated with the activation of *N*-methyl-D-aspartate (NMDA) receptors (Newell et al., 1997). The altered levels of glutamate and glycine indicated that BaP might affect the regulation of nerve signal transduction in the digestive gland.

Taurine and homarine are vital organic osmolytes in marine mollusks (Tikunov et al., 2010; Zhang et al., 2011a). BCAAs function as osmolytes and are involved in osmotic regulation in marine invertebrates. Therefore, the presence of disordered osmolytes suggests that osmotic stress in the digestive gland was induced by BaP exposure.

In the present study, the differential changes in various amino acids, glucose, ATP, and some osmolytes indicate that short-duration exposure to BaP disturbed osmoregulation, energy metabolisms, and nerve signal transmission in the digestive gland tissue of *P. martensii*.

#### 3.2.2. Effects of BaP on the metabolome of the gills

For metabolites of the gills, the low concentration of BaP induced significant increases in alanine, glutamate, glucose, and ATP levels and

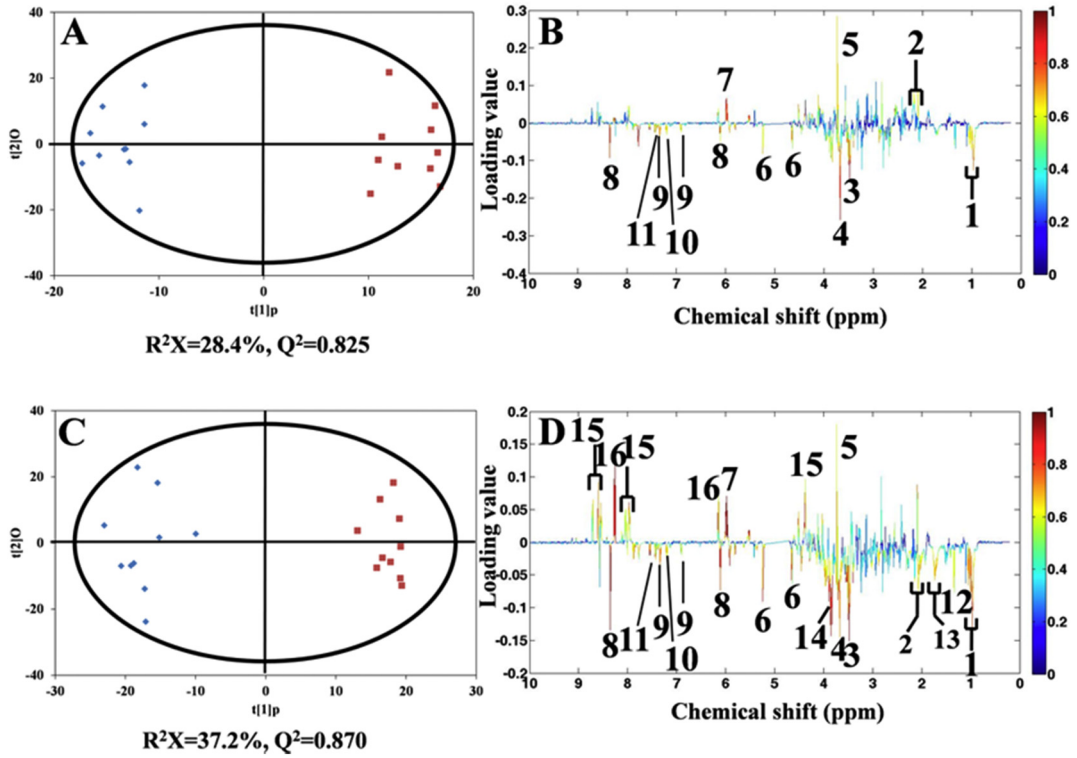


**Fig. 1.** OPLS-DA scores derived from the $^{1}$H NMR spectra of digestive gland extracts from the solvent control (♦) and BaP-treated groups (■) after exposures for 72 h to (A) 1 and (C) 10 μg/L of BaP and the corresponding coefficient plots (B) and (D). The color map shows the significance of the metabolite variations between the two classes (solvent control and BaP treatments). Peaks in the positive direction indicate metabolites that are more abundant in the BaP-exposed groups. Alternatively, metabolites that are more abundant in the solvent control group are presented as peaks in the negative direction.
Keys: 1. BCAAs (valine, leucine and isoleucine), 2. Glutamate, 3. Taurine, 4. Glycine, 5. Unknown 1 (3.62 ppm), 6. Glucose, 7. Unknown 2 (5.96 ppm), 8. Inosine, 9. Tyrosine, 10. Histidine, 11. Phenylalanine, 12. Threonine, 13. Arginine, 14. Unknown 3 (3.82 ppm), 15. Homarine and 16. ATP.

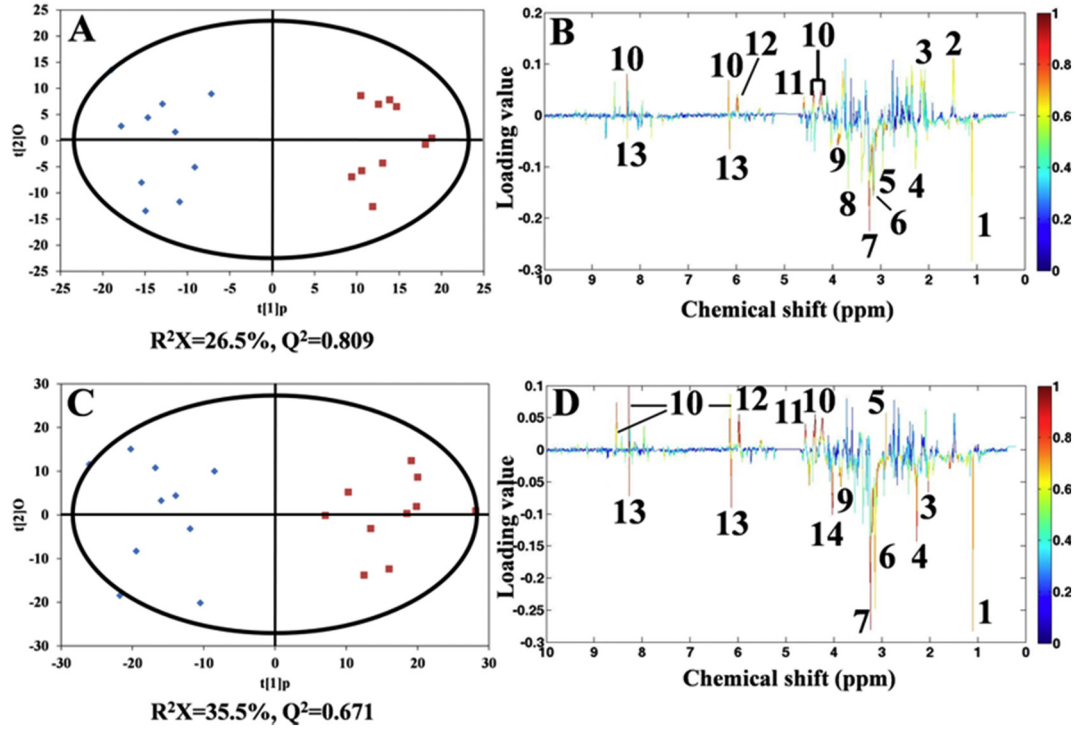


**Fig. 2.** OPLS-DA scores derived from the $^{1}$H NMR spectra of gill extracts from solvent control (♦) and BaP-treated groups (■) after exposures for 72 h, (A) 1 μg/L and (C) 10 μg/L of BaP and the corresponding coefficient plots (B) and (D). The color map shows the significance of the metabolite variations between the two classes (solvent control and BaP treatments). Peaks in the positive direction indicate metabolites that are more abundant in the BaP-exposed groups. Alternatively, metabolites that are more abundant in the solvent control group are presented as peaks in the negative direction.
Keys: 1. Unknown 1 (1.10 ppm), 2. Alanine, 3. Glutamate, 4. Acetoacetate, 5. Dimethylglycine, 6. Malonate, 7. Phosphocholine, 8. Glycine, 9. Betaine, 10. ATP, 11. Glucose, 12. Unknown 2 (5.96 ppm), 13. Inosine and 14. Unknown 3 (4.02 ppm).

**Table 1**
The differentially expressed metabolites ($P < 0.05$[a]) in the digestive gland and gill tissues of *P. martensii* exposed to 1 μg/L and 10 μg/L BaP for 72 h.

| Digestive gland | | Gill | |
|---|---|---|---|
| 1 μg/L BaP | 10 μg/L BaP | 1 μg/L BaP | 10 μg/L BaP |
| Osmotic regulation: | Osmotic regulation: | Osmotic regulation: | Osmotic regulation: |
| BCAAs↓ | BCAAs↓ | Alanine↑ | |
| Taurine↓ | Taurine↓ | Dimethylglycine↓ | Dimethylglycine↑ |
| | Homarine ↑ | Betaine↓ | Betaine↓ |
| Glycine↓ | Glycine↓ | Glycine↓ | |
| Energy metabolism: | Energy metabolism: | Energy metabolism: | Energy metabolism: |
| Tyrosine ↓ | Tyrosine ↓ | Phosphocholine↓ | Phosphocholine↓ |
| Histidine↓ | Histidine↓ | Acetoacetate↓ | Acetoacetate↓ |
| Phenylalanine↓ | Phenylalanine↓ | Malonate ↓ | Malonate ↓ |
| Glucose↓ | Glucose↓ | Glucose↑ | Glucose↑ |
| Inosine↓ | Inosine↓ | Inosine↓ | Inosine↓ |
| Glutamate↑ | ATP↑ | ATP↑ | ATP↑ |
| | Arginine↓ | Glutamate↑ | Glutamate↓ |
| | Threonine↓ | | |
| | Glutamate↓ | | |
| neurotransmitter: | | neurotransmitter: | |
| Glutamate↑ | Glutamate↓ | Glutamate↑ | Glutamate↓ |
| Glycine↓ | Glycine↓ | Glycine↓ | |

↑: Significantly up-regulated metabolites involved in various physiological functions.
↓: Significantly down-regulated metabolites involved in various physiological functions.
a. *P*-values determined using one-way ANOVA on the bin areas from the representative peak of the corresponding metabolite.

significantly reduced acetoacetate, dimethylglycine, malonate phosphocholine, glycine, betaine, and inosine levels. High concentration of BaP caused an increase in the levels of dimethylglycine, ATP, and glucose. While causing a decrease in glutamate, acetoacetate, malonate, phosphocholine, betaine, and inosine levels (Fig. 2 and Table 1).

Dimethylglycine and betaine are known to act as osmolytes that play an important roles in osmotic regulation (Viant et al., 2003; Ji et al., 2014). The level of dimethylglycine was affected by the change in the glycine level (Wu and Wang, 2010). The alteration in the levels of glycine, dimethylglycine and betaine suggested that BaP induced osmotic stress in the gill tissue. Alanine is involved in anaerobic metabolism and is a small organic osmolyte that is present in marine bivalves (Preston, 1993). Thus, increase in the alanine level is a potential indicator of short-duration exposure to a low dose of BaP.

Malonate, acetoacetate, and phosphocholine are involved in some energy metabolic pathways. Malonate, which is a key enzyme in the tricarboxylic acid (TCA) cycle, competes with succinate and is a competitive inhibitor of cellular respiration (Zhang et al., 2011a). The decreased malonate level indicates that BaP most likely affects the TCA cycle associated with energy metabolism in the gills. Additionally, acetoacetate is a type of ketone body that is produced from acetyl-coenzyme A (acetyl-CoA). The significantly decreased acetoacetate level indicates that lipid metabolism was weakened in the gills exposed to BaP. Further, phosphocholine is catalyzed by choline kinase, which converts choline and ATP into ADP and phosphocholine (Liu et al., 2014). Thus, the reduced phosphocholine level implies that BaP induced an increase in the energy demand in the gills. Additionally, changes in phosphocholine level may be associated with toxicants-induced oxidative stress, reactive oxygen species production, and lipid peroxidation, which may potentially alter cellular membrane stability (Brandão et al., 2015). Consequently, BaP might disrupt the gill cellular membrane stability by changing the phosphocholine levels, and induce the neurotoxicity of gill cells by altering the levels of glycine and glutamate.

In the present study, the changes in the levels of these metabolites imply that a short-duration exposure to BaP might disturb energy metabolism, nerve signal transmission, and osmotic regulation in the gill tissue of *P. martensii*. These results agreed with previous research, which revealed that 10 μg/L of BaP could disturb osmotic regulation in the gill tissue of *Perna viridis* (Song et al., 2016).

### 3.2.3. Effects of BaP on the physiological functions of the two tissues

The differentially expressed metabolites are involved in various physiological functions in the digestive gland and gill tissues exposed to the two doses (1 μg/L and 10 μg/L) of BaP for 72 h (Table 1). Most metabolites that exhibited changes following BaP exposure were involved in energy metabolisms, osmotic regulation, and nerve signal transmission. However, different metabolites induced changes in various metabolic pathways in the two tissues of *P. martensii*. Specifically, BaP mainly caused energy metabolism-related changes by altering amino acid levels in the digestive gland tissue. In the gill tissue, BaP disrupted energy metabolism, as demonstrated by the depletion in phosphocholine, acetoacetate, and malonate levels.

## 4. Conclusions

In summary, NMR-based metabolomics revealed metabolic changes in the digestive glands and gills after 72 h of BaP exposure. These results indicated that BaP can induce tissue-specific metabolic responses in the digestive gland and gill tissues of *P. martensii*. In details, a high concentration of BaP disturbed energy metabolism and promoted osmotic stress, while a low concentration of BaP accelerated the energy deterioration and disturbed osmotic regulation in the digestive gland tissue. Both concentrations of BaP disturbed osmotic regulation and energy metabolism in the gill tissue. BaP was found to be able to induce neurotoxicity in both tissues. In addition, it was found that some tissue-specific metabolites can be used as the potential biomarkers to indicate BaP contamination.

Supplementary data to this article can be found online at https://doi.org/10.1016/j.marpolbul.2018.03.057.

## Acknowledgement

The research was funded by the National Natural Science Foundation of China (31160126, 41161077). We thank the editors and the anonymous reviewers for their valuable comments and suggestions on the article.

## References

Banni, M., Hajer, A., Sforzini, S., Oliveri, C., Boussetta, H., Viarengo, A., 2014. Transcriptional expression levels and biochemical markers of oxidative stress in *Mytilus galloprovincialis* exposed to nickel and heat stress. Comp. Biochem. Physiol. C:

Toxicol. Pharmacol. 160, 23–29.
Binelli, A., Riva, C., Cogni, D., Provini, A., 2008. Assessment of the genotoxic potential of benzo(a)pyrene and pp'-dichlorodiphenyldichloroethylene in Zebra mussel (*Dreissena polymorpha*). Mutat. Res. 649, 135–145.
Brandão, F., Cappello, T., Raimundo, J., Santos, M.A., Maisano, M., Mauceri, A., Pacheco, M., Pereira, P., 2015. Unravelling the mechanisms of mercury hepatotoxicity in wild fish (*Liza aurata*) through a triad approach: bioaccumulation, metabolomic profiles and oxidative stress. Metallomics: Integrated Biometal Science 7, 1352–1363.
Canesi, L., Barmo, C., Fabbri, R., Ciacci, C., Vergani, L., Roch, P., Gallo, G., 2010. Effects of vibrio challenge on digestive gland biomarkers and antioxidant gene expression in *Mytilus galloprovincialis*. Comp. Biochem. Physiol. C: Toxicol. Pharmacol. 152, 399–406.
Cappello, T., Mauceri, A., Corsaro, C., Maisano, M., Parrino, V., Lo Paro, G., Messina, G., Fasulo, S., 2013. Impact of environmental pollution on caged mussels *Mytilus galloprovincialis* using NMR-based metabolomics. Mar. Pollut. Bull. 77, 132–139.
Cappello, T., Brandao, F., Guilherme, S., Santos, M.A., Maisano, M., Mauceri, A., Canario, J., Pacheco, M., Pereira, P., 2016a. Insights into the mechanisms underlying mercury-induced oxidative stress in gills of wild fish (*Liza aurata*) combining (1)H NMR metabolomics and conventional biochemical assays. Sci. Total Environ. 548-549, 13–24.
Cappello, T., Pereira, P., Maisano, M., Mauceri, A., Pacheco, M., Fasulo, S., 2016b. Advances in understanding the mechanisms of mercury toxicity in wild golden grey mullet *(Liza aurata)* by $^{1}$H NMR-based metabolomics. Environ. Pollut. 219, 139–148.
Chen, H., Song, Q., Diao, X., Zhou, H., 2016. Proteomic and metabolomic analysis on the toxicological effects of benzo[a]pyrene in pearl oyster *Pinctada martensii*. Aquat. Toxicol. 175, 81–89.
Chiu, K.H., Dong, C.D., Chen, C.F., Tsai, M.L., Ju, Y.R., Chen, T.M., Chen, C.W., 2017. NMR-based metabolomics for the environmental assessment of Kaohsiung Harbor sediments exemplified by a marine amphipod (*Hyalella azteca*). Mar. Pollut. Bull. 124 (2), 714–724.
Dorts, J., Kestemont, P., Thezenas, M.L., Raes, M., Silvestre, F., 2014. Effects of cadmium exposure on the gill proteome of Cottus gobio: modulatory effects of prior thermal acclimation. Aquat. Toxicol. 154, 87–96.
Fasulo, S., Iacono, F., Cappello, T., Corsaro, C., Maisano, M., D'Agata, A., Giannetto, A., De Domenico, E., Parrino, V., Lo Paro, G., Mauceri, A., 2012. Metabolomic investigation of *Mytilus galloprovincialis* (Lamarck 1819) caged in aquatic environments. Ecotoxicol. Environ. Saf. 84, 139–146.
Feng, J., Li, J., Wu, H., Chen, Z., 2013. Metabolic responses of HeLa cells to silica nanoparticles by NMR-based metabolomic analyses. Metabolomics 9 (4), 874–886.
Fernandez-Tajes, J., Florez, F., Pereira, S., Rabade, T., Laffon, B., Mendez, J., 2011. Use of three bivalve species for biomonitoring a polluted estuarine environment. Environ. Monit. Assess. 177, 289–300.
Ji, C., Wei, L., Zhao, J., Wu, H., 2014. Metabolomic analysis revealed that female mussel *Mytilus galloprovincialis* was sensitive to bisphenol A exposures. Environ. Toxicol. Pharmacol. 37, 844–849.
Knecht, A.L., Truong, L., Simonich, M.T., Tanguay, R.L., 2017. Developmental benzo[a]pyrene (B[a]P) exposure impacts larval behavior and impairs adult learning in zebrafish. Neurotoxicol. Teratol. 59, 27–34.
Liu, X., Zhang, L., You, L., Yu, J., Zhao, J., Li, L., Wang, Q., Li, F., Li, C., Liu, D., Wu, H., 2011. Differential toxicological effects induced by mercury in gills from three pedigrees of Manila clam *Ruditapes philippinarum* by NMR-based metabolomics. Ecotoxicology 20, 177–186.
Liu, X., Ji, C., Zhao, J., Wang, Q., Li, F., Wu, H., 2014. Metabolic profiling of the tissue-specific responses in mussel *Mytilus galloprovincialis* towards *Vibrio harveyi* challenge. Fish Shellfish Immunol. 39, 372–377.
Liu, Y., Chen, T., Li, M.H., Xu, H.D., Jia, A.Q., Zhang, J.F., Wang, J.S., 2015. (1)H NMR based metabolomics approach to study the toxic effects of dichlorvos on goldfish (*Carassius auratus*). Chemosphere 138, 537–545.
Newell, D.W., Barth, A., Ricciardi, T.N., Malouf, A.T., 1997. Glycine causes increased excitability and neurotoxicity by activation of NMDA receptors in the hippocampus. Exp. Neurol. 145, 235–244.
Newsholme, P., Procopio, J., Lima, M.M., Pithon-Curi, T.C., Curi, R., 2003. Glutamine and glutamate–their central role in cell metabolism and function. Cell Biochem. Funct. 21, 1–9.
Phillips, D.H., 1999. Polycyclic aromatic hydrocarbons in the diet. Mutat. Res. 443, 139–147.
Preston, R.L., 1993. Transport of amino acids by marine invertebrates. J. Exp. Zool. 265, 410–421.
Santacroce, M.P., Pastore, A.S., Tinelli, A., Colamonaco, M., Crescenzo, G., 2015. Implications for chronic toxicity of benzo[a]pyrene in sea bream cultured hepatocytes: cytotoxicity, inflammation, and cancerogenesis. Environ. Toxicol. 30, 1045–1062.
Shi, Y., Yu, C., Gu, Z., Zhan, X., Wang, Y., Wang, A., 2013. Characterization of the pearl oyster (*Pinctada martensii*) mantle transcriptome unravels biomineralization genes. Mar. Biotechnol. 15, 175–187.
Song, Q., Chen, H., Li, Y., Zhou, H., Han, Q., Diao, X., 2016. Toxicological effects of benzo (a)pyrene, DDT and their mixture on the green mussel *Perna viridis* revealed by proteomic and metabolomic approaches. Chemosphere 144, 214–224.
Speciale, A., Zena, R., Calabro, C., Bertuccio, C., Aragona, M., Saija, A., Trombetta, D., Cimino, F., Lo Cascio, P., 2018. Experimental exposure of blue mussels (*Mytilus galloprovincialis*) to high levels of benzo[a]pyrene and possible implications for human health. Ecotoxicol. Environ. Saf. 150, 96–103.
Tikunov, A.P., Johnson, C.B., Lee, H., Stoskopf, M.K., Macdonald, J.M., 2010. Metabolomic investigations of American oysters using H-NMR spectroscopy. Mar. Drugs 8, 2578–2596.
Tuffnail, W., Mills, G.A., Cary, P., Greenwood, R., 2008. An environmental 1H NMR metabolomic study of the exposure of the marine mussel *Mytilus edulis* to atrazine, lindane, hypoxia and starvation. Metabolomics 5, 33–43.
Tung, E.W., Philbrook, N.A., Belanger, C.L., Ansari, S., Winn, L.M., 2014. Benzo[a]pyrene increases DNA double strand break repair in vitro and in vivo: a possible mechanism for benzo[a]pyrene-induced toxicity. Mutat. Res. Genet. Toxicol. Environ. Mutagen. 760, 64–69.
Viant, M.R., 2007. Metabolomics of aquatic organisms: the new ' omics' on the block. Mar. Ecol. Prog. Ser. 332, 301–306.
Viant, M.R., Rosenblum, E.S., Tjeerdema, R.S., 2003. NMR-based metabolomics: a powerful approach for characterizing the effects of environmental stressors on organism health. Environ. Sci. Technol. 37, 4982–4989.
Wang, H., Cui, L., Cheng, H., Zhang, Y., Diao, X., Wang, J., 2017. Comparative studies on the toxicokinetics of benzo[a]pyrene in *Pinctada martensii* and *Perna viridis*. Bull. Environ. Contam. Toxicol. 98, 649–655.
Watanabe, M., Meyer, K.A., Jackson, T.M., Schock, T.B., Johnson, W.E., Bearden, D.W., 2015. Application of NMR-based metabolomics for environmental assessment in the Great Lakes using zebra mussel (*Dreissena polymorpha*). Metabolomics 11, 1302–1315.
Wills, L.P., Jung, D., Koehrn, K., Zhu, S., Willett, K.L., Hinton, D.E., Di Giulio, R.T., 2010. Comparative chronic liver toxicity of benzo[a]pyrene in two populations of the Atlantic killifish (*Fundulus heteroclitus*) with different exposure histories. Environ. Health Perspect. 118, 1376–1381.
Wu, H., Wang, W.X., 2010. NMR-based metabolomic studies on the toxicological effects of cadmium and copper on green mussels *Perna viridis*. Aquat. Toxicol. 100, 339–345.
Wu, H., Southam, A.D., Hines, A., Viant, M.R., 2008. High-throughput tissue extraction protocol for NMR- and MS-based metabolomics. Anal. Biochem. 372, 204–212.
Xie, J., Zhao, C., Han, Q., Zhou, H., Li, Q., Diao, X., 2017. Effects of pyrene exposure on immune response and oxidative stress in the pearl oyster, *Pinctada martensii*. Fish Shellfish Immunol. 63, 237–244.
Yan, C., Wu, W., Li, H., Zhang, G., Duerksen-Hughes, P.J., Zhu, X., Yang, J., 2010. Benzo [a]pyrene treatment leads to changes in nuclear protein expression and alternative splicing. Mutat. Res. 686, 47–56.
Zhang, L., Liu, X., You, L., Zhou, D., Wang, Q., Li, F., Cong, M., Li, L., Zhao, J., Liu, D., Yu, J., Wu, H., 2011a. Benzo(a)pyrene-induced metabolic responses in Manila clam *Ruditapes philippinarum* by proton nuclear magnetic resonance ((1)H NMR) based metabolomics. Environ. Toxicol. Pharmacol. 32, 218–225.
Zhang, L., Liu, X., You, L., Zhou, D., Wu, H., Li, L., Zhao, J., Feng, J., Yu, J., 2011b. Metabolic responses in gills of Manila clam *Ruditapes philippinarum* exposed to copper using NMR-based metabolomics. Mar. Environ. Res. 72, 33–39.